A Digital-geometry-based Framework used in an Omnidirectional Laser-Optics Technology for Inspecting Pipes

Abbasali Dehghan Tezerjani[1], Mehran Mehrandezh[2] and Raman Paranjape[2]

[1]Inuktun Service Ltd., Nanaimo, Canada,
[2]Faculty of Engineering and Applied Science, University of Regina, Regina, Canada
mehran.mehrandezh@uregina.ca

_____

ABSTRACT

This paper presents a novel method for inspecting the interior surface of pipes using laser-optics. The variation in the local curvature of a laser ring projected onto the pipe's surface is measured via an image taken by an omnidirectional camera, hence the name omnidirectional laser optics. There will be sharp changes in the curvature when the laser ring passes over defects (i.e., dents, cracks, sliver, bad weld trims, etc.). Computationally-traceable digital-geometry-based metrics are used to calculate the change in curvature through an elliptical curve fitting in real time. Experimental results prove the high performance of the proposed method for detecting small defects at a high resolution and in a short time.

Key words: Laser-optics, digital geometry, curvature estimation from image, omnidirectional cameras and opto-mechatronics
_____

INTRODUCTION

Automated surface inspection of pipes refers to a class of methods and algorithms which detect, classify, localize and measure surface defects on the interior surface of the pipes. Different sensors like vision, sonar, radiography-based, and thermal are used for pipe inspection. In this paper, we propose a laser-optics sensor for detecting external and visible defects. The literature on image-based inspection of pipes is vast. Duran et al. used a perspective camera and laser ring pattern projector for visual inspection of small sewer pipes ([6] and [7]). They used a pinhole camera to image the LED ring light projected onto the pipe surface, and then used artificial Neural Networks for analyzing the brightness of the LED ring to detect the defects. This method was used to detect large defects only.

Our survey leads us to believe that the image-based inspection of sewer pipes has been mainly used by small field-of-view perspective camera. Because of the small FOV in the pinhole perspective cameras, it is not practical to use them for inspecting large pipes. Therefore, alternative imaging systems with a wide field of view (FOV) would be required to make the imaging of the entire interior surface of the pipes possible. There are three main approaches for panoramic imaging of the interior surface of a pipe: multiple camera system, rotary imaging platform ([9]) and omnidirectional imaging system. Multiple-camera and rotary-imaging systems can capture the pipe surface with higher resolution than that in omnidirectional imaging systems. However, because of the difficulties in image feature bundle adjustment, image stitching and mosaicking, multiple view calibration and also synchronization of the imaging systems, they have been rarely successful. Further-more, the overall cost of these systems is prohibitive. In this paper, we focus on visual inspection of the interior surface of pipes using single-view omnidirectional imaging sensors. Single-view Omnidirectional imaging can be categorized as: Catadioptric and Dioptric. Both can be used for capturing panoramic view of the scene in one single image. A catadioptric sensor consists of a perspective camera and a hyperbolic or parabolic mirror. Dioptric imaging sensors, on the other hand, consist of a camera with a compound lens (*e.g.*, a fish- eye lens) with about 180-degree horizontal and vertical field of views. This would enable the camera to see a hemisphere lobe in front of it.

In this paper, we investigate defect detection on the interior surface of pipes using a laser ring, projected onto the pipe's inner wall, and an omnidirectional imaging system. Furthermore, one can benefit from the simplicity, the compact size, and wide FOV of these sensors. However, lower resolution and higher distortion in images are two main drawbacks of using omnidirectional sensors.

There are some works on visual inspection of pipes using omnidirectional sensors cited in the literature ([3] and [14]). Matsui *et al* ([14]) used the omnidirectional camera and laser light for the digital reconstruction of the interior surface of the pipes. Their main focus is on the design of the optical system, thus, they do not address the defect detection in depth.

Two main approaches widely used for illuminating the pipe wall in pipe inspection applications are: *diffused* and *structured* light. The former uses a high-intensity yet the diffused light source, where the latter adopts a collimated structured light using laser. There are different mechanisms for generating structured light patterns in machine vision, namely, laser pattern projectors and image fringes generated by the common data projectors. The laser projectors create a single-wavelength high contrast pattern of the laser light, whereas the data projectors project a multi-wavelength light (aka, image fringe) at a lower intensity and contrast. Although data projectors have the advantage of creating a dynamic range of patterns on the fly, but because of the lower intensity and contrast that they offer, and also the bigger size factor, they have been rarely used in industry. Recent developments on imaging sensors and actuators under the MEMS/NEMS, though, can be a game changer. Basu *et al* [3] and Inari *et al* [11] used the laser ring projector to create a narrow ring on the interior surface of a pipe.

In this research, we used a high-intensity laser line projector as the lighting subsystem to produce a highly focused illumination inside the pipe. Rather than using laser ring projectors with a low fan angle which makes the inspection of large diameter pipes a serious challenge, we use the laser line projector laterally and perpendicular to the pipe surface to produce a laser ring inside the pipe right next to the camera. In this laser-optics imaging system, an elliptical curve is formed within the image whose size and form would depend on the relative position/orientation (aka, pose) of the laser optics imaging system inside the pipe. The curve generated by the laser line projector is the best source of information about the surface defects inside the pipe. Every surface defect would locally change the curvature of the laser line. The main idea is to extract and analyze these local changes in curvature in the elliptical curve seen in the image to detect, classify, localize and measure surface defects on the interior surface of the pipe.

There are two main approaches for extracting defect information from the projected curve on the interior surface of the pipe: *fixed reference* and *dynamic reference*. The first method uses a recorded or a priori registered no-defect curve as the reference (or signature) curve to find the part of the instantaneous curve which is distorted by the defect. In this approach, one can easily calculate the differences between the reference (or signature) curve and the instantaneous curve in order to find defects. On the other hand, in the dynamic- reference method, one does not need to memorize any reference, but finds the defects using local curvature c h a n g e s on every frame instantaneously. A static-reference approach would be advantageous if the laser-optics sensing unit moves smoothly inside the pipe. However, in scenarios where the sensing unit might sway in motion, then a dynamic-referencing approach would yield more accurate results.

In this work, we use *a dynamic reference approach* for extracting surface defects from the projected curve, which further helps us to develop the algorithms robust to t h e robot's unwanted sway in motion. In our proposed method, we formulate a novel algorithm to track the local changes in the curvature of the elliptical shape of the laser line in the image to find defects. It is noteworthy, however, that a- prior knowledge of the curve's geometry can drastically help in tracking discontinuity in the local curvature, which will be described in further details.

In this paper, we present a novel approach for the surface inspection of big pipes using omnidirectional imaging sensors and a laser projector based on digital-geometry-based elliptical curve fitting and local curvature extraction. We did several experiments on the steel and PVC pipes. Results were promising. The proposed algorithm could detect small defects of 2 mm width or larger. We present the system set up for our pipe inspection method in the next section. Then, we describe the defect detection method in detail. Finally, we present a brief discussion about the method and our results.

SYSTEM SETUP

Every machine vision application consists of two main components: imaging and lighting subsystems. Appropriate selection of these two components highly affects the performance of the machine vision applications. The lighting system should be selected in a way that it will highlight features of interest. On the other hand, the main objective of the imaging subsystem is to see and captured highlighted features at the highest resolution.

In this work we chose omnidirectional vision as the imaging component and a green laser line projector as the illumination subsystem. Fig. 1 shows the schematic of our imaging/lighting platform as well. We used the green laser line projector as the light source to produce a high intensity/contrast image of the scene. The laser projector produces a thin line of green light which produces a circular ring on the interior surface of the pipe. This ring will be seen as an ellipse in the image. Fig. 1 shows the elliptical curve as well. Also, it should be noted that there are some alternative solutions, e.g. the laser ring projector or the Axicon lenses [17], for projecting the narrow laser ring inside the pipe. But because of the complexity of the setup and implementation, they were not considered.
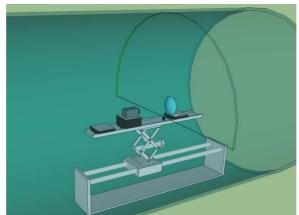
Fig. 1 The schematic of the proposed setup of the omnidirectional laser-optics imaging system for pipe inspection

There are some design factors to be considered in an omnidirectional laser optics system. The lighting system, in particular, must provide the highest visibility and resolution. For instance, the laser line should be seen close to the boundary of the image for the highest resolution. It has been experimentally verified that for achieving the highest longitudinal and depth resolutions, the laser ring must be projected onto the pipe surface right above the reflective mirror in Catadioptric imaging systems. This means that the projected laser line will be reflected through the mirror's periphery in the Catadioptric sensors and fish-eye lens's periphery in the Dioptric sensors. As one can see in Fig. 1, laser line projector is projecting a beam perpendicular to optical axis of the camera and close to the periphery of the   mirror.

The main characteristics of the proposed design are as follows:
- Overlapped central axis of the camera and the mirror
- Adjustable relative position of the laser line projector
- Adjustable elevation of the camera and the mirror
- Adjustable relative position of the camera and the mirror

METHODOLOGY

In this section, we present a set of algorithms used for defect detection in pipes using the proposed omnidirectional laser-optics platform consisting of an omnidirectional imaging sensor and a laser line projector. We use the definition of local curvature to do elliptical curve fitting on the boundary of the projected laser curve on the interior surface of the pipe and then detect and extract defect parts by calculating the difference between the measured boundary from the image and its elliptical fit.

Fig. 2 shows the flowchart of the defect extraction algorithm presented in this paper. We start by capturing the image and then applying a dynamic-threshold algorithm to extract the laser light projected curve. The details of this method will be described in the next section. In the next step, we extract upper and lower boundaries of the curve (i.e., considering the thickness of the laser line). If some discontinuities were found on the image we fix it in the digital image by stitching all the corresponding curve boundary segments together to make a pair of complete boundary curves (pre-processing the image data). After pre-processing the boundaries, we apply a point-filtering algorithm on the curve boundary points. After filtering unwanted points on the curve boundary, due to the noise in the image, we fit two elliptical shape curves to each side of the boundary. Finally, we compare fitted ellipses to the curve boundaries with the original images to extract the position and size of the defects. In the following, further details on each module in the aforementioned flowchart are provided.

Dynamic Thresholding
After capturing the image, the very first task is to extract the laser light projected curve from the image. ae converted the RGB images to a grey-level for simplicity, since what matters the most in our algorithm would be the light intensity and not the colour. Also, in the next immediate step, we converted from a grey-level to a BW image in a way that all points on the laser projected curve are highlighted.

Because of the non-uniform distribution of the laser light intensity on the surface of the pipe, a simple global thresholding method, which applies the same threshold for all image pixels, may not work. However, the following observation can be made on the intensity profile of the laser line: the intensity of the light decreases as the polar angle to the central axis of the laser projector and/or the distance to the laser's projection center increases. Assuming that the laser projector is perfectly aligned with the pipe's central axis, one can conclude that the intensity would change only radially. This helped us to design a dynamic-reference thresholding algorithm that would account for non-uniform intensity profile along the curve.

We modelled the radial intensity variation using a third-order polynomial to adjust the average intensity of each pixel in the image of the curve. Fig. 3 shows the polynomial model of the laser intensity along the curve. A third-order polynomial will provide a smooth change in the intensity that can be calculated in a very short   time.

A comparison between our dynamic-reference thresholding and static-reference thresholding methods was done through experiments and former proved to work better. Fig. 4 shows a representative comparison between the dynamic- vs static-reference thresholding. As can be seen, low values of the threshold cause some light diffusion be counted as part of the curve, whereas high values chosen for the threshold would entirely disregard low-illumination part of the curve. On the contrary, the dynamic-reference thresholding method, not only keeps low illumination parts intact, but also it removes spattered light diffusion found at the centre of the   curve.

Effect of the Big Defects on the Boundary Extraction

It is a fairly straightforward process to extract curve boundaries from the image. For example, simple column-wise scanning of the foreground pixels will find the boundaries. However, in case of big defects, the diffusion of laser light on the defect can cause some irregularities such as discontinuities on the curve boundaries which should be addressed carefully. Fig. 5 shows the effect of the big-size defects on the boundary of the curve.
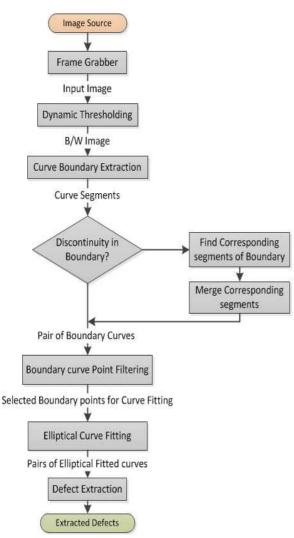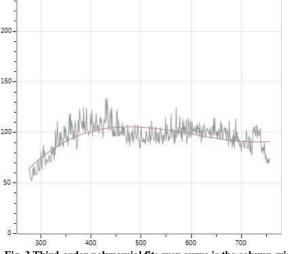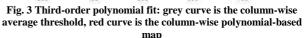

Fig. 3 Third-order polynomial fit: grey curve is the column-wise average threshold, red curve is the column-wise polynomial-based map

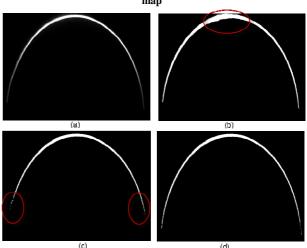**Fig. 2 Flowchart of the proposed defect extraction algorithm**

Fig. 4 Static- vs. Dynamic-reference Threshold a) Original image b) static-reference threshold at t=30 c) static-reference threshold at t=80 d) Dynamic-reference threshold

To deal with this problem, firstly we apply a size filter to remove all the small islands on the image which are far enough from the other connected components of the image. These islands usually correspond to the light distortion at the defected position that would not provide any valid information on the defect size or shape. The filtering adopted here is based on the following information obtained on the islands in the image:

- Size of the island
- Roundness of the island.
- Distance to closest connected component neighbour.

_____

The weights to be adopted on each factor can be learned through experiments and/or a machine-learning algorithm. After filtering the unwanted islands, we apply the merge algorithm which merges adjacent curve segments. To do the merge operation, we check the points on both ends of each curve segment to find corresponding pairs and then do the merge. We repeat the merge operation until all the curve segments are merged to the two lower and upper boundary curves. Fig. 6 shows the result of the boundary merge process. As shown in this figure, unwanted islands are filtered out prior to the merge process and then remaining components are merged to the upper and lower boundaries.
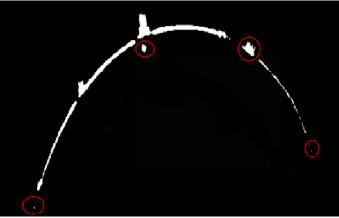

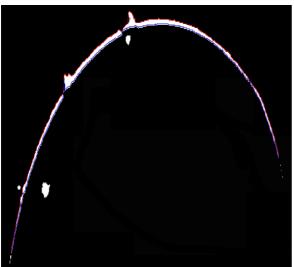**Fig. 5 Effect of the big-size defects on the boundary of the light curve**

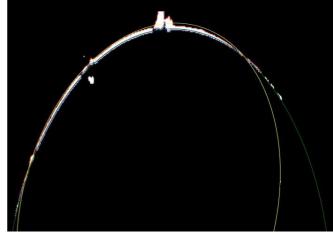
Fig. 6 Merged points on the boundary curves

Fig. 7 Effect of the defect points on deviation of the fitted ellipse: red: upper boundary points, blue: lower boundary points, yellow: the fitted ellipse to the upper boundary green: the fitted ellipse to the lower boundary
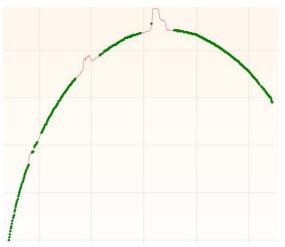

Fig. 8 Result of the point filtering algorithm applied to the upper boundary curve seen in fig. 6 red: original boundary curve green: points remained after filtering
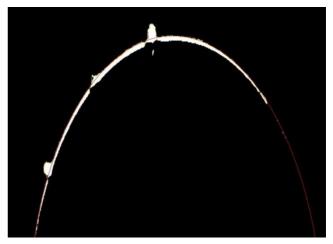

Fig. 9 Result of the ellipse fitting algorithm applied on the filtered upper boundary curve yellow: filtered points on boundary curve red: the fitted ellipse

Point Filtering on Boundary Curves

After extracting upper and lower boundary curves, we fit an elliptical curve to each boundary. For each boundary curve, there will be two classes of points. In the first class, the points correspond to the non-defect areas of the pipe. These points preserve the smoothness of the fitted curve. In the second class, however, the points correspond to the defect areas. These points violate the smooth bending in the fitted curve. They can shift the fitted elliptical curve by large away from non-defect points. Fig. 7 show the deviation of the fitted ellipse caused by the points on the defect area. As one can see in this figure, yellow ellipse which is fitted to the upper boundary curve is deviated from the non-defect points on the upper boundary because of including defect points to the curve fitting process. This necessitates devising an efficient algorithm for excluding the major defect points from the fitting process.

To resolve the aforementioned problem, we pre-filter the major defect points by adopting a local curvature calculation originally proposed by Marji ([13]). In fact, there are many different definitions for the local curvature of the digitized curves. Local curvature can be estimated using one of the following criteria:

- The change in the slope angle of the tangent line (*e.g.*, relative to the x-axis).
- The derivatives along the curve.
- The radius of the osculating circle (also called circle of curvature).

Majdi [13] fitted binomial curves to any point, and its immediate neighbouring points, on the digitized curve and then used derivative of them to calculate the local curvature. Also Hermann et al [15] used maximum-length 8DSS, [5], definition on bi-lateral sides of any point p on the digitized curve to calculate the local curvature at that point.

In this work, we calculate the local curvature of every point along the digitized curve using the method cited in [13] and then filter out the boundary points using the following two metrics:

- Points with high local curvature value.
- Points with high fluctuation in the local curvature in their vicinity.

In fact, all the points violating the smoothness of the curve will be removed through this process prior to implementing the next step, namely ellipse fitting. Fig. 8 shows the result of the filtering algorithm applied to the points on the upper boundary as seen in Fig. 7. In this figure, green points correspond to the points which are not filtered. As we can see in this figure, using the aforementioned simple rules can correctly reject all of the defect points. One can also optimize the design parameters in the local curvature rejection hypothesis via experimentation. These parameters would affect the overall sensitivity of the algorithm to the local fluctuation on the curve. They would also affect the filtering process. However, it should be noted that false rejection of a few points along the curve would not affect the final results by large, given that only 6 points are necessary to fit an ellipse to the laser image boundaries. In the next subsection we will discuss the fitting process in details.

Ellipse Fitting

Projection of the laser on the interior surface of the pipe would be seen as a smooth elliptical curve in the image under ideal conditions. It can be a perfect circle, if the laser was perfectly aligned with the pipe centre line, otherwise the curve would have an elliptical shape. The best fitted elliptical curve can be then used as a reference (or signature) curve to find and extract all the defects. In general, one can represent an ellipse in the form of a quadratic equation:

$$a x^2 + b y^2 + c x y + d x + e y + f = 0 \qquad (1)$$

In this equation $< x, y >$ are the coordinates of the ellipse points in a 2D space. By having 6 different points on the ellipse, one can uniquely determine the coefficients a to f using least-square-error fitting algorithm. There are three main approaches for the ellipse fitting to a set of data points: *Algebraic Fitting* (8) and [10], *Orthogonal Least Square Fitting* [2] and [1], and *Maximum Likelihood* [4] and [12].

In this paper, we used the algebraic fitting method proposed by Hal et al [10]. It represents a non-iterative least square minimization method which guarantees an ellipse-specific solution even for scattered or noisy data. Fig. 9 shows the fitted ellipse to the filtered upper and lower boundaries of the curve as well. As shown in this figure, the algorithm efficiently finds the best ellipse fit to the filtered point of the curve boundaries. After finding the reference ellipse for upper and lower boundaries of the light curve, we have to detect the defects by finding the difference between the reference ellipse and original boundary points.

Defect Extraction

As discussed earlier, we eliminate the defected points from the boundary curves in the image to find a precise elliptical fit to the non-defected points. Now this elliptical-fit curve can be used to extract defected points at a higher resolution. We refer to this as a *cascaded filtering strategy*.

To detect and extract the defects on the boundary curve, we calculate the distance from the original boundary points to their corresponding points on the ellipse based on: *Vertical* and *Radial displacements*.

Let us suppose that $p = <x_p, y_p>$ is a point on the boundary curve. We define the vertical displacement of this point as:

$$d_v(p) = \|p - p_v\| \qquad | \ x_{p_v} = x_p \ \wedge \ p_v \in Ellipse \qquad (2)$$

In fact, the vertical displacement of point p is a Euclidean distance from the point p to the corresponding point on ellipse having the same x coordinates. We also define the radial displacement of the point p as:

$$d_r(p) = \|p - p_r\| \qquad | \ \frac{y_{p_r}-y_c}{x_{p_r}-x_c} = \frac{y_p-y_c}{x_p-x_c} \ \wedge \ p_r \in Ellipse \qquad (3)$$

In this equation $c = <x_c, y_c>$ is the center point, or the point in the middle of two pivot points of the ellipses fit to the lower and upper boundaries. As one can see in this equation, the corresponding radial point is the point on the ellipse with the same orientation of the boundary point ellipse p relative to the center of the ellipse c. Fig. 10 depicts the vertical and radial displacement as well. Comparing these two shows that although the vertical resolution is much simpler to calculate, the error in calculation increases as the point p goes far from the center of the ellipse.

One can calculate the displacement profile as the profile of the displacement of the points on the boundary curves. It can be used as the input data for defect detection and extraction. We define the defected region as a set of consecutive points on the profile which have the displacement error larger than a user-defined specific threshold value. We use this threshold value to filter out small displacements calculated along the profile, which basically correspond to the noise in the image rather than a defect (i.e., light fluctuation due to reflection/refraction). Fig. 11 shows the radial profile of the boundary curve. As shown in this figure, radial displacement criteria find the defected points effectively. In the next section, we present some representative experimental results on surface inspection of the PVC and steel pipes. Defects could be detected, and separated from image noise, with a high confidence.
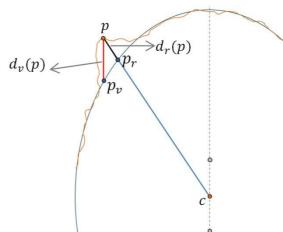

Fig. 10 Result of the ellipse fitting algorithm applied on the filtered upper boundary curve yellow: filtered points on boundary curve red: the fitted ellipse
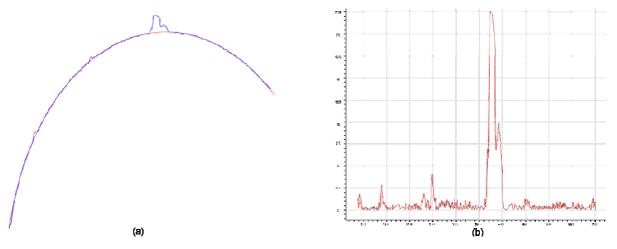

Fig. 11 Radial profile of the boundary curves extracted using fitted ellipse. a) Boundary curve and corresponding fitted ellipse b) The radial profile of the boundary curve

DISCUSSION

In this section, we discuss some outstanding issues around the proposed algorithm as a design   guideline.

Omnidirectional vs. Pinhole Perspective Imaging System
In this work, we used the omnidirectional imaging sensor instead of perspective camera for imaging 360 degree inside the pipe. The main drawback of the omnidirectional sensors is the high image distortion and lower resolution. However, for larger pipes, the resolution in omnidirectional imaging systems can be comparable to that in perspective imaging systems. We applied our algorithm on a 24-inch PVC pipe. Our experiments showed that the resolution of the omnidirectional sensor   used was good enough to detect defects about 2mm in width or larger. Fig. 12 illustrates detection of a 2mm crack on the surface of 24 inch PVC pipe as well. Our studies show that the accuracy of the imaging system, when using the proposed algorithm, is good enough for the quality control of the pipes.

Catadioptric vs. Dioptric Sensors
As mentioned earlier, the proposed algorithm is applicable to both Catadioptric and Dioptric sensors. These systems were experimentally tested in our lab. One can conclude that distortion of the image in the Dioptric imaging systems (a camera with a fisheye lens) is higher for the points on the periphery of the image. However, Dioptric imaging sensors are more compact in size and easier to calibrate due to the fewer number of moving parts. Also, they would provide a higher resolution than that in the Catadioptric imaging sensors with the same focal length. In conclusion, for the applications where 3D reconstruction of the scene is needed, because of the low distortion at the periphery of the image, the Catadioptric sensors would be preferable. For defect detection purposes, when no metrology is needed. However, a dioptric imaging sensor would be advantageous.

Dynamic Thresholding
In this paper, we presented a column-wise dynamic-reference thresholding method in order to compensate for intensity changes in the laser light projected onto the interior surface of a pipe in the image. Results show major improvement in the quality of the extracted binary image. We used a third order polynomial to model the light intensity changes along the curve.

Point Filtering of the Boundary Curves
We used the local curvature information to filter out defected points on the lower/upper boundary curves in the image before fitting elliptical curves to them. Throughout this process, false removal of a few non-defected points would not affect the final result by large. This helps us fit the elliptical curves faster and more efficiently. This would be in particular useful for conducting real-time inspection of pipes.

Real-Time Surface Inspection
In every machine vision application time complexity of the image processing algorithms plays an important role. In this work we applied five main steps to extract the defects on the boundary of the curve (See Fig. 2). Table 1 show the time complexity associated with each step of the proposed method. As can be seen, except the dynamic-reference threshold algorithm which needs to scan all the image pixels with a time complexity of $O(n^2)$, the remaining steps in the proposed algorithm can be executed in a linear time, simply because they just process the pixels on the boundary points and not the entire image. It should be also noted that we also extract all the white points on the image in a specific generic list, which would further help us to do all other steps in the proposed algorithm linear time.
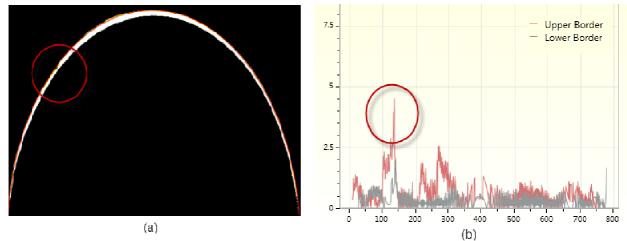

Fig. 12 Detection of a 2mm crack on the surface of 24 inch PVC pipe. a) Boundary curve and corresponding fitted ellipse b) Radial displacement profile of the boundary curves

Comparing the proposed algorithm with other Fixed reference frame methods, shows that the overall time complexity of the algorithm doesn't change and one can use this approach in real-time as well.

Table -1 Time Complexity of the Main Steps on the Proposed Surface Inspection Algorithm

Dynamic Thresholding	$O(n^2)$
Boundary Extraction	$O(n)$
Point Filtering	$O(n)$
Ellipse Fitting	$O(n)$
Defect Extraction	$O(n)$

CONCLUSION

We presented a novel approach for surface inspection of pipes using a laser-optics technology that consists of an omnidirectional imaging sensor and a collimated laser line projected onto the pipe's wall. We used a green laser line projector to highlight a very thin ring inside the pipe, and fitted two elliptic curves to the lower and upper boundaries of the image of this laser ring. These curves were used as two signature curves for detecting defects. We concluded:

- Despite the fact that the overall spatial resolution pro- vided by the Catadioptric and Dioptric imaging sensors is lower than that in the perspective cameras ([16]), they provide a compact and cost-effective solution for panoramic imaging of pipes of any size. Furthermore, a high resolution can be also achieved through an optimal configuration setup.
- Structured light can highlight defects better than the diffused light. However, the light intensity of the laser, projected onto the pipe wall, can change radially. We proposed a dynamic-thresholding technique to compensate for the light intensity variations in the projected laser ring. Further tuning would be required to discriminate the defects from image noise. The mathematical tools used in this method can be tuned via machine learning.
- Calculating the variation of the local curvature along the lower/upper boundaries of the structured light can identify defects. After some nominal tuning of the parameters, we were able to detect defects with a high confidence. This algorithm could separate the image noise from real defects with a low computational cost that is required in real-time applications.

REFERENCES

[1] SJ Ahn, W Rauh and HJ Warnecke, Least-Squares Orthogonal Distances Fitting of Circle, Sphere, Ellipse, Hyperbola and Parabola, Pattern *Recognition*, **2001**, 34(12), 2283–2303.

[2] S J Ahn, W Rauh, H S Cho and HJ Warnecke, Orthogonal Distance Fitting of Implicit Curves and Surfaces, *IEEE Transactions on Pattern Analysis and Machine Intelligence,* **2002**, 24(5),620–638.

[3] A Basu and D Southwell, Omni-Directional Sensors for Pipe Inspection, *IEEE International Conference on Systems, Man and Cybernetics, Intelligent Systems for the 21st Century*, **1995**, 4, 3107 –3112.

[4] W Chojnacki, M Brooks, A Van Den Hengelo and D Gawley, On the Fitting of Surfaces to Data with Covariances, *IEEE Transactions on Pattern Analysis and Machine Intelligence*, **2000,** 22(11), 1294– 1303.

[5] D Coeurjolly and R Klette, A Comparative Evaluation of Length Estimators of Digital Curves, *IEEE Transactions on Pattern Analysis and Machine Intelligence*, **2004,** 26(2), 252 –258.

[6] O Duran, K Althoefer and L Seneviratne, Automated Sewer Pipe Inspection through Image Processing, *IEEE International Conference on Robotics and Automation ICRA*, **2002**, 3, 2551–2556.

[7] O Duran, K Althoefer and LD Seneviratne, Pipe Inspection using a Laser-Based Transducer and Automated Analysis Techniques, *IEEE/ASME Transactions on Mechatronics,* **2003,** 8(3), 401 –409.

[8] A Fitzgibbon, M Pilu and R Fisher, Direct Least Square Fitting of Ellipses, *IEEE Transactions on Pattern Analysis and Machine Intelligence,* **1999,** 21(5), 476–480.

[9] C Frey, Rotating Optical Geometry Sensor for Fresh Water Pipe Inspection, *IEEE Sensors,* **2008**, 337–340.

[10] R Hal and J Flusser, Numerically Stable Direct Least Squares Fitting of Ellipses, *The Sixth International Conference in Central Europe on Computer Graphics and Visualization*, **1998,** 21(5), 125–132.

[11] T Inari, K Takashima, M Watanabe and J Fujimoto, Optical Inspection System for the Inner Surface of a Pipe using Detection of Circular Images Projected by a Laser Source, Measurement, **1994**, 13(2), 99–106.

[12] Y Leedan and P Meer, Heteroscedastic regression in computer vision: problems with bilinear constraint, *International Journal of Computer Vision*, **2000**, 37(2), 127–150.

[13] M Marji, *On the Detection of Dominant Points on Digital Planar Curves*, PhD Thesis, Wayne State University, Detroit, Michigan, **2003.**

[14] K Matsui, A Yamashita and T Kaneko, 3-D Shape Measurement of Pipe by Range Finder Constructed with Omnidirectional Laser and Omnidirectional Camera, *IEEE International Conference on Robotics and Automation (ICRA)*, **2010**, 2537–2542.

[15] RK Simon Hermann, Multigrid Analysis of Curvature Estimators, *Proceeding of Image Vision Computing New Zealand*, **2003**, 108–112

[16] AD Tezerjani, M Mehrandezh and R Paranjape, Optimal Spatial Resolution of Omnidirectional Imaging Systems for Pipe Inspection Applications, *International Journal of Optomechatronics*, **2015**, (in press).

[17] *http://fpopticsarizonaedu/opti696/2005/axicon_ Proteedf.*